

Available online at www.sciencedirect.com

Marine Chemistry xx (2006) xxx–xxx

**MARINE
CHEMISTRY**

www.elsevier.com/locate/marchem

Barium cycling along WOCE SR3 line in the Southern Ocean

S.H.M. Jacquet^{a,c,*}, F. Dehairs^a, M. Elskens^a, N. Savoye^a, D. Cardinal^b

^a *Vrije Universiteit Brussel-Analytical and Environmental Chemistry Department-Pleinlaan 2, B-1050 Brussels, Belgium*

^b *Royal Museum for Central Africa-Department of Geology-B-3080 Tervuren, Belgium*

^c *Centre d'Océanologie de Marseille, Laboratoire d'Océanographie et de Biogéochimie, Marseille, France*

Received 7 October 2005; received in revised form 30 March 2006; accepted 19 June 2006

Abstract

Spring and summer profiles of dissolved and particulate barium (Ba) from WOCE SR3 line (145°E) in the Southern Ocean are compared and seasonal evolutions discussed. Fluxes are estimated from mass conservation equations and from differences in reservoir contents between seasons. Subtraction of barium is observed at mesopelagic depths (upper 600 m) and appears to exceed up to tenfold the combined local build-up and the deep-ocean fluxes of particulate Ba, pointing towards significant dissolution to take place in intermediate and deep waters. Although regression analyses identify silicate as the major predictor of dissolved Ba, Ba and silicate are clearly uncoupled in surface waters where Ba behaves more similar to nitrate, excluding diatoms as users of Ba. Moreover, we observe a southward decrease in the Ba vs. silicate regression slopes driven by the conditions in intermediate and deep waters and mainly marked by the location of the Polar Front. These findings corroborate existing knowledge about the predominant control by barite formation and dissolution on the oceanic Ba cycle. It suggests a decreased dissolution of barite south of the Polar Front as compared to the situation in the Polar Front Zone and the Subantarctic Zone. This is in agreement with the fact that, except for deep waters, the Antarctic Circumpolar Current water column is oversaturated with respect to barite, in contrast to the situation north of the Polar Front, where the whole water column is undersaturated [Jeandel C., B. Dupré, G. Lebaron, C. Monnin and J.F. Minster, 1996. Longitudinal distributions of dissolved barium, silica and alkalinity in the western and southern Indian Ocean. *Deep-Sea Res. I*, 43 (1), 1–31; Monnin, C., C. Jeandel, T. Cattaldo and F. Dehairs, 1999. The marine barite saturation state of the world's ocean. *Mar. Chem.*, 65, 253–261].

© 2006 Elsevier B.V. All rights reserved.

Keywords: Southern Ocean; Ba-nutrients; Ba-alkalinity relationship; Dissolved and particulate barium dynamics

1. Introduction

Although the oceanic distribution of dissolved barium (Ba_d) shows strong similarities with those of silicate and alkalinity (likely indicating an uptake linked to planktonic activity), the biogeochemical cycling of Ba appears uni-

que (Chan et al., 1977; Lea and Boyle, 1989; Lea, 1993; Jeandel et al., 1996; Jacquet et al., 2005a,b), involving a strong link with the Ba-barite (BaSO₄) dynamics. Barite precipitation inside biogenic aggregates has been proposed as the main mechanism of biogeochemical Ba subtraction (Dehairs et al., 1980; Stroobants et al., 1991) in a World Ocean mostly undersaturated for BaSO₄ (Monnin et al., 1999; Rushdi et al., 2000). Inside such micro-environments, Ba subtraction from solution, release of biogenic Ba or oxidation of organic sulfur was put forward as the probable processes leading to supersaturation of

* Corresponding author. Vrije Universiteit Brussel-Analytical and Environmental Chemistry Department-Pleinlaan 2, B-1050 Brussels, Belgium. Tel.: +32 2 629 39 70; fax: +32 2 629 32 74.

E-mail address: sjacquet@vub.ac.be (S.H.M. Jacquet).

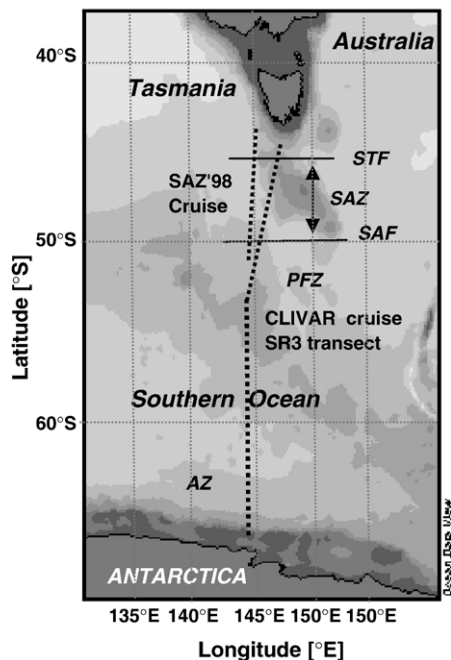


Fig. 1. Geographical setting of the study areas during the SAZ'98 (summer 1998) and CLIVAR SR3 (spring 2001) cruises along WOCE SR3 line in the Australian sector of the Southern Ocean (~ 145°E).

barite (Collier and Edmond, 1984; Bertram and Cowen, 1997; Dehairs et al., 2000; Ganeshram et al., 2003). The association of barite formation with bacterial degradation of organic matter followed by release of discrete barite micro-crystals in the ambient water, led to use discrete barite crystals as an indirect proxy for mesopelagic mineralization of exported biogenic material (Dehairs et al., 1997; Cardinal et al., 2005). Studies by González-Muñoz et al. (2003) have shown that barite production may be directly bacterially mediated and suggest that bacteria may enhance barite production by providing nucleation sites for crystal growth. Alternative pathways, in the surface layer, involve the incorporation of Ba in the celestite (SrSO_4) skeleton of acantharians and active barite precipitation during skeleton dissolution (Bernstein et al., 1998; Bernstein and Byrne, 2004). However, work by Esser and Volpe (2002) and Ganeshram et al. (2003) argues against acantharians as the main source of biogenic barium in the upper water column. Experimental work on diatom cultures has shown Ba-uptake in diatoms to be relatively small and insufficient to sustain the Ba contents and fluxes in the deeper ocean (Dehairs et al., 1980; Sternberg et al., 2005b). Thus, the peculiar distribution of dissolved Ba in the water column appears conditioned mainly through the formation and dissolution of

biogenic barite, but the 100- to 1000-fold larger concentrations of dissolved Ba compared to particulate Ba render it difficult to quantify possible effects of non-conservative processes on the dissolved phase.

The Southern Ocean is characterised by strong seasonal modulations mainly linked to hydrodynamic forcing and biogeochemical gradients along fronts (Arrigo et al., 1998; Landry et al., 2002). This environment is of particular interest to study the dependency of Ba on biological activity, export from the surface layers and hydrodynamics. Recently, Jacquet et al. (2005b) studying the frontal system of the Crozet Kerguelen Basin (Indian sector of the Southern Ocean) underpinned the fact that the Ba distribution does not depend on the same particle–solute interaction processes which control alkalinity and silicate. While such results are in line with the fact that formation and dissolution of barite are major processes shaping the oceanic Ba profile, they did not provide clear evidence that barite formation does measurably influence the distribution of dissolved Ba.

Here we present dissolved and particulate Ba profiles obtained for spring and summer situations during two cruises along the WOCE SR3 line (145°E), crossing the Southern Ocean south of Tasmania from the Subtropical Zone to the Polar Front Zone. We confront dissolved Ba with physico-chemical conditions and investigate the correlative behavior of Ba with nutrients (silicate and nitrate) and alkalinity via multiple regression analysis, in order to

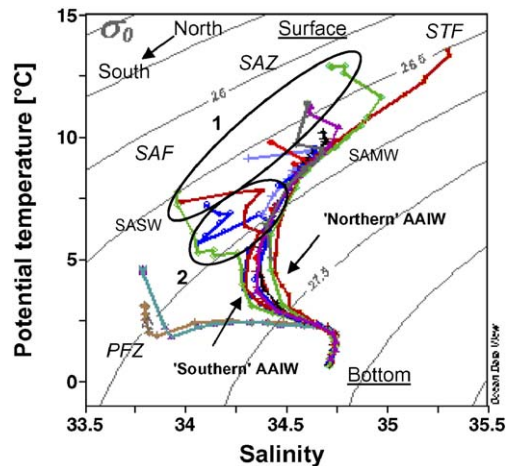


Fig. 2. Potential temperature–salinity plots and isopycnals for SAZ'98 and CLIVAR SR3 profiles. STF=Subtropical Front, SAZ=Subantarctic Zone, SAF=Subantarctic Front, PFZ=Polar Front Zone, SAMW=Subantarctic Mode Water, SASW=Subantarctic Surface Water, AAIW=Antarctic Intermediate Water. 1=northward advection of cold and fresh surface waters; 2=strong variability in SAF subsurface waters due to cross-frontal exchanges. Graph constructed using Ocean Data View (Schlitzer R., 2003; Ocean Data View; <http://www.awi-bremerhaven.de/GEO/ODV>).

improve our understanding of the biogeochemical processes involved in shaping the nutrient-like distribution of dissolved Ba. Then we estimate the subtraction of dissolved Ba in subsurface and mesopelagic waters during the growth season and compare this subtraction with release of particulate Ba and with Ba fluxes in deep waters.

2. Materials and methods

Dissolved Ba (Ba_d) and particulate Ba (Ba_p) were studied in the Australian sector of the Southern Ocean along north–south transects between Tasmania and Antarctica (Fig. 1). For the Subtropical, Subantarctic and Polar Front Zones, we confront data for summer 1998 (SAZ'98 cruise, AU9706; February–April) and spring

2001 (CLIVAR-SR3 cruise, AU0103; October–December). The CLIVAR-SR3 Ba_d transect is the most resolved spatially (depth, latitude), with 32 stations and 24 depths sampled from the Subtropical Zone (STZ) to the Antarctic Zone (AZ). The entire Ba_d data set for CLIVAR-SR3 is discussed in Jacquet et al. (2004). Dissolved Ba data for the SAZ'98 cruise have not been published previously. The particulate Ba data sets for SAZ'98 and CLIVAR-SR3 are discussed in Cardinal et al. (2001, 2005), respectively. During SAZ'98, we sampled eight sites for dissolved Ba and four for particulate Ba in the area between the Subtropical Front and the Polar Front Zone. During CLIVAR-SR3, the same area was sampled with 24 sites for dissolved and 3 for particulate Ba. Stations suitable for comparing spring (CLIVAR-SR3) and summer situations

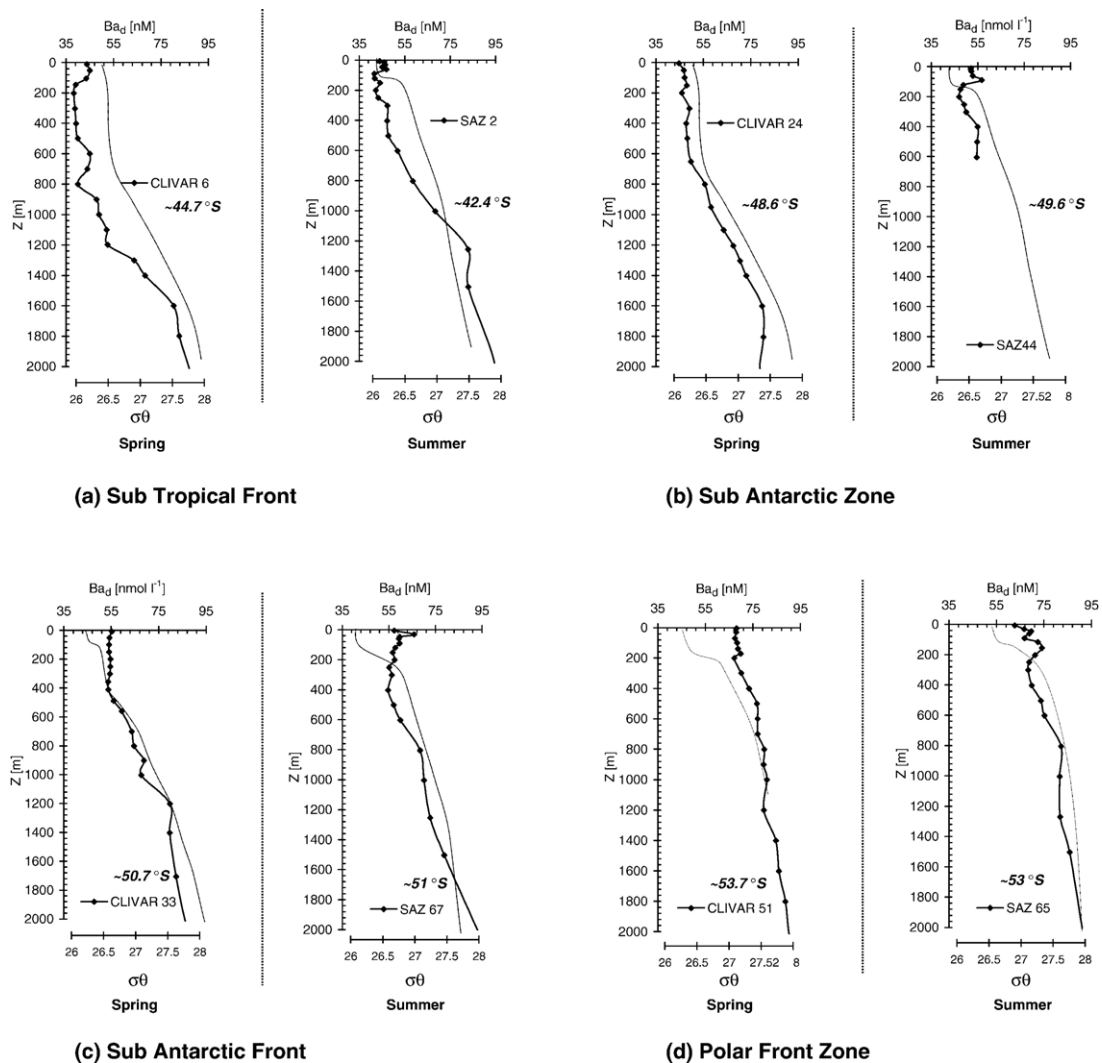


Fig. 3. Dissolved Ba (nM) in the upper 2000 m water column during spring (CLIVAR-SR3 cruise, 2001) and summer (SAZ'98 cruise, 1998), shown together with profiles of potential density (thin dotted curve, kg m^{-3}). Station numbers refer to original CTD cast numbers.

(SAZ'98) were selected on the basis of potential temperature–salinity properties (Tpot-S diagram, Fig. 2). Dissolved and particulate Ba profiles were not obtained from the same CTD casts, but from casts sampled close by in time and space and having similar Tpot-S data profiles. Deep carbon and Ba export fluxes discussed here are from Trull et al. (2001b) and Cardinal et al. (2005), respectively. Six sediment traps were deployed between September 1997 and February 1998, in the Subantarctic Zone (46.8°S at 1060, 2050 and 3850 m), the Subantarctic Front (51°S at 3089 m) and the Polar Front Zone (53.8°S at 830 and 1580 m). Ba fluxes were corrected for trapping efficiency via excess ^{230}Th (Trull et al., 2001b; Cardinal et al., 2005). Salinity, temperature and nutrients data from CTD bottles have been provided by Marc Rosenberg (Rosenberg et al., unpublished report) and alkalinity data (for CLIVAR-SR3 only) by Bronte Tilbrook (CSIRO, Hobart).

Data for CLIVAR-SR3 and SAZ'98 are taken to represent spring (2001) and summer (1998) conditions, respectively. The evolution of the monthly averaged Chl-a contents for the period 1997 to 2006, based on SEAWIFS imagery, reveals a quite regular pattern from year to year with onset of the bloom in September and demise towards March–April (Rathbone and Griffiths, 2006). Inter-annual variation in timing of onset and demise of seasonal plankton development did not exceed 3 weeks. Furthermore, the evolution of the 2001–2002 growth season is consistent with observations on seasonal Chl-a evolution reported by Trull et al. (2001a,b) for the 1997–1999 period. Therefore, for comparison purposes, we consider that the timing of the season's onset and progress was similar throughout the period 1998 to 2001. We also assume that 100 days have elapsed between spring and summer.

2.1. Hydrological setting

The investigated sections cross the Subtropical Front (STF), the Subantarctic Zone (SAZ), the Subantarctic Front (SAF) and the Polar Frontal Zone (PFZ) (Figs. 1 and 2). Detailed descriptions of the complex physical structure of the area, circulation, water masses and fronts are given in Rintoul and Bullister (1999), Trull et al. (2001a) and Sokolov and Rintoul (2002). Briefly, the main hydrodynamical features observed during both cruises are the following (see Tpot-S diagram, Fig. 2): (1) the SAZ and SAF are characterized by cool and fresh surface waters (upper 100 m; circle 1 in Fig. 2); (2) below the surface layer in the SAF, there is strong variability in the Tpot-S plots reflecting interleaving processes (circle 2 in Fig. 2); (3) in the sub-surface layers between STF and SAF a continuum of

Antarctic Intermediate Waters (AAIW) is observed showing decreasing salinities and temperatures from north to south (the northern variety is of Tasman Sea origin; Rintoul and Bullister, 1999); (4) PFZ stations clearly differentiate from the areas to the north, with very fresh and cold waters at potential densities > 27.5 .

2.2. Analysis

Dissolved barium was measured using an isotope dilution inductively coupled plasma quadrupole mass spectrometry method (ID-ICP-MS) as described by Klinkhammer and Chan (1990) and Freydier et al. (1995). This method was adapted for application on a VG PlasmaQuad 2+ analytical instrument by adding neodymium as internal standard to correct for mass bias (Navez et al., 1999; Jacquet et al., 2005b). Sensitivity of the ICP-MS instrument was 20,000 to 25,000 cps (counts per second) for $1 \mu\text{g l}^{-1} \text{ }^{138}\text{Ba}$. Blank signals (Milli-Q grade water) fluctuated between 50 to 100 cps and the detection limit is $\sim 3 \text{ ng l}^{-1}$. Dissolved Ba concentrations in Southern Ocean seawater samples diluted 30-fold range from 0.3 to $0.5 \mu\text{g l}^{-1}$ of Ba. Reproducibility of our method is $\pm 1.5\%$ (RSD) as tested on repeat preparations of unknowns and reference solutions (SLRS-3 and 'OMP', the latter an in-house Mediterranean Sea water prepared by C. Jeandel, OMP, LEGOS, Toulouse; France). Samples preparation is as follows: 1 ml of seawater is spiked with 0.7 to 1 ml of a ^{135}Ba -spike solution (93.8% ^{135}Ba) to produce a $^{138}\text{Ba}/^{135}\text{Ba}$ ratio around 0.7 (Klinkenberg et al., 1996). Then 0.3 ml of a 69.3 nM Nd solution with natural $^{146}\text{Nd}/^{143}\text{Nd}$ abundance is added. Finally, the sample is diluted 30-fold with Milli-Q grade water. Quantities of sample, spikes and dilution water were accurately assessed by weighing.

The detailed procedure for particulate Ba is given in Cardinal et al. (2001). Briefly, particulate material was completely digested in sealed Teflon beakers using a hot HF/HCl/HNO₃ mixture. Ba contents were measured by ICP-AES and ICP-MS. Reproducibility of particulate Ba measurements is $\pm 2.5\%$ (RSD). Biogenic Ba (hereafter

Table 1
Spring and summer mesopelagic Ba_d (a, nM) and Ba_{xs} (b, pM) depth weighted average values; integration between 100 and 600 m

Location	STF	SAZ	SAF	PFZ
<i>(a) Mesopelagic dissolved Ba (nM)</i>				
Spring	47.9	55.3	58.7	77.1
Summer	46.1	52.0	56.7	73.6
<i>(b) Mesopelagic particulate Ba (pM)</i>				
Spring	–	221	223	305
Summer	328	393	487	516

called excess Ba or Ba_{xs}) was calculated by subtracting the lithogenic Ba from total Ba. Lithogenic Ba was estimated from the Al content and a Ba/Al molar ratio of 0.00135 for the upper continental crust, taken as representative for the lithogenic material in suspended matter (Taylor and McLennan, 1985). The lithogenic Ba fraction was minor to negligible and the fraction of Ba_{xs} accounted for $\geq 95\%$ of total Ba. Furthermore, earlier studies (Dehairs et al., 1980; Stroobants et al., 1991) indicate that the Ba_{xs} in oceanic suspended matter consists mainly of micron-sized crystalline barite.

3. Results— Ba_d and Ba_{xs} distributions

Spring (CLIVAR-SR3) and summer (SAZ'98) Ba_d profiles are reported in Fig. 3 for representative stations from the STF to PFZ together with potential density

profiles. Summer dissolved Ba profiles present similar latitudinal and vertical trends as spring profiles (the latter from Jacquet et al., 2004). Ba_d gradients between the surface and 2000 m range from 40 to 80 nM (STF), 45–50 to 80 nM (SAZ), 50–60 to 80 nM (SAF) and 65–70 to 90 nM (PFZ). Deeper in the water column (data not shown here), concentrations increase and values reach up to 110 nM and more in bottom waters at 4000 m. Overall, these SR3 data sets compare well with data reported for other cruises in the Southern Ocean (Chan et al., 1977; Östlund et al., 1987; Poisson et al., 1990; Jeandel et al., 1996; Jacquet et al., 2005b).

Summer Ba_d profiles show more variability than spring profiles in the upper 600 m (Fig. 3), with slight depletions extending over the mesopelagic zone at the STF and the PFZ. The depth where a density gradient sets the lower boundary of the surface mixed layer

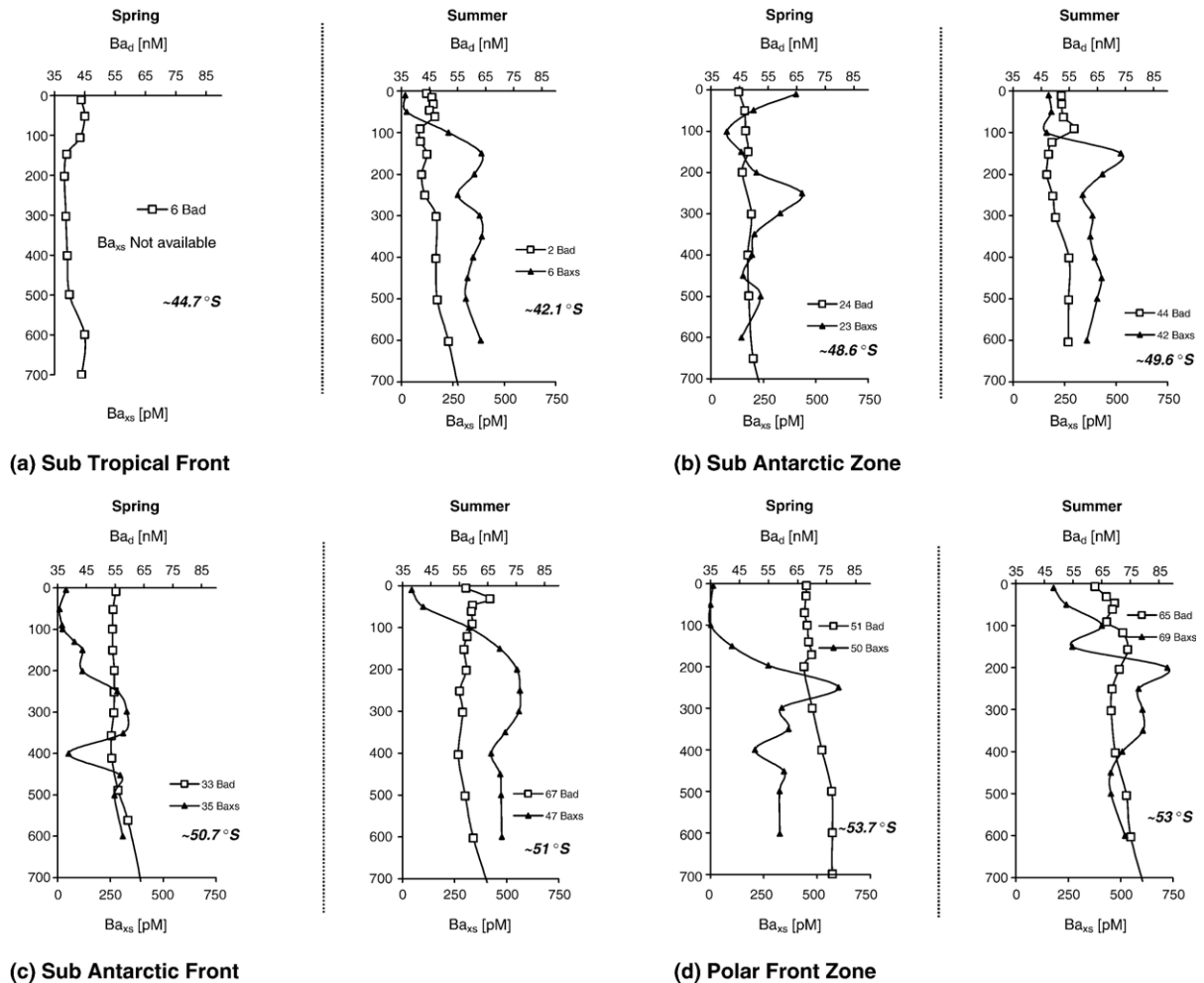


Fig. 4. Profiles of dissolved Ba (open squares, nM) and particulate Ba (closed triangles, pM) profiles during spring (CLIVAR-SR3 cruise, 2001) and summer (SAZ'98 cruise, 1998) in the upper 700 m water column. Station numbers refer to original CTD cast numbers.

generally coincides with the depth where summer Ba_d concentrations start to decrease. For both seasons, we integrated Ba_d profiles between 100 and 600 m (depth weighted average value; Table 1a) and summer mesopelagic Ba_d values are systematically lower than spring values. Subsurface depletions are usually not observed for the spring Ba_d profiles (Fig. 3) except for a slight depletion in the STF where the Ba_d profile is probably influenced by the complex frontal system in the upper 1000 m (Jacquet et al., 2004).

Fig. 4 shows corresponding dissolved and particulate Ba profiles in the upper 700 m during spring and summer. Ba_{xs} concentrations tend to rise on from the depth where a density gradient sets the lower boundary of the surface mixed layer (Figs. 3 and 4). Ba_{xs} profiles display maxima between 100 and 350 m which reach higher values in summer compared to spring (Table 1b; see also Cardinal et al., 2005).

4. Discussion

The precise mechanism shaping the nutrient-like distribution of Ba_d is still debated and this is partly due to the complexity of the processes leading to formation of barite, a major player in the oceanic Ba cycle. Even if, at first, Ba and silicate $Si(OH)_4$ are not expected to be coupled, similarities of their distributions tend to indicate control via direct Ba uptake by marine planktonic organisms (Chan et al., 1977, Lea, 1993, Jeandel et al., 1996; see discussion further below). However, except for a cultured unicellular Prymnesiophyte alga (*Exanthemachrysis gayraliae*; Fresnel et al., 1979) and for Acantharians, which are celestite ($SrSO_4$) secreting micro-heterotrophs (Bernstein et al., 1998; Bernstein and Byrne, 2004; Sternberg et al., 2005a), no other marine pelagic plankton group has been reported to be involved in Ba uptake and barite formation. Indeed, experimental work has shown that production of barite is induced during phytoplankton aggregation and subsequent mineralization (Ganeshram et al., 2003), corroborating hypotheses issued earlier (Bishop, 1988; Dehairs et al., 1991). Both possible main barite formation loci (Acantharians and decaying plankton) are not just limited to the upper mixed layer but are likely to occur mainly in waters below as shown by the unique feature of Ba_p profiles, i.e. an increase in the mesopelagic layers. The scenario involving aggregation–mineralization appears as being the most consistent with an ubiquitous occurrence of the Ba_{xs} maximum in the mesopelagic waters (e.g. Dehairs et al., 1991, 1997; Cardinal et al., 2001, 2005). Confronting dissolved and particulate Ba distributions could be a means to identify

the strata where the Ba uptake occurs. This is, however, a difficult task considering the 100- to 1000-fold larger concentration of dissolved compared to particulate Ba, which renders it difficult to quantify possible impacts of nonconservative processes on the dissolved phase. In order to understand such effects and the involvement of dead plankton processing on the Ba dynamics, we investigate the correlative behavior of dissolved Ba with nutrients (silicate and nitrate) and alkalinity and then with particulate biogenic Ba.

4.1. Dissolved barium behaviour in the water column

4.1.1. Correlative behaviour of barium with nutrients and alkalinity

Inspecting the barium vs. silicate and alkalinity regressions in intermediate and deep waters ($\sigma_\theta > 27.35$) reveals strong correlations. For the region north of the PF, the Ba-silicate correlation is consistent between the SAZ'98 (1998) and the CLIVAR-SR3 (2001) cruises indicating little year to year variability (see circled part 4 in Fig. 5). Focusing on the whole CLIVAR-SR3 data set, which includes the Antarctic Zone south of the PF (see Jacquet et al., 2004), we observe the slope of the Ba vs. Si regression to decrease southward (Fig. 6). In contrast, in surface and mesopelagic waters where the action of nutrient uptake takes place ($\sigma_\theta < 27.35$, ~ upper 600 m, see circled parts 2 and 3 in Fig. 5), the picture (for both cruises) is quite different. Barium and silicate now appear uncoupled, with Ba concentrations remaining high, while silicate reaches depletion (note that the silicate depletion extends more southward in summer compared to spring). In the upper 600 m, silicate subtraction appears as a major process but it does not affect Ba. Ba_d and nitrate, on the contrary, appear to covary but Ba never reaches depletion, while nitrate does (see circled part 1 in Fig. 5). Since Ba in surface waters is uncoupled from silicate, diatoms appear not to consume Ba, at least not in a constant proportion to Si. This is in agreement with observations from laboratory experiments indicating that cultured diatoms do not incorporate barium in significant amounts (see Dehairs et al., 1980 and recent work of Sternberg et al., 2005b). Furthermore, the upper 600 m of water column between STZ and PFZ is characterized by an inverse relationship between Ba and alkalinity (see circled part 1 in Fig. 7), a feature we also observed in the Indian sector of the Southern Ocean (Jacquet et al., 2005b) and which reflects the uncoupling of both these parameters. Millero et al. (1998) showed that this latitudinal surface gradient for alkalinity is mainly controlled by evaporation.

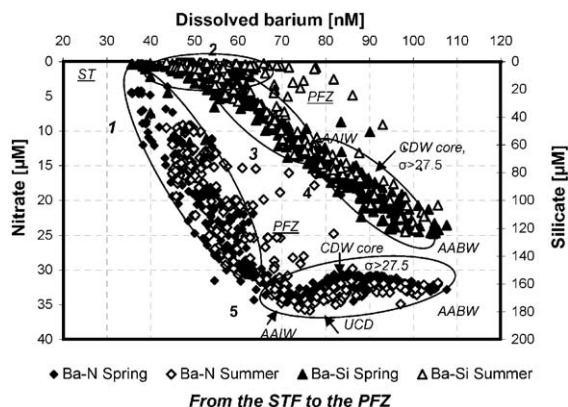


Fig. 5. Dissolved Ba (nM) versus nutrients (silicate and nitrate, μM) for CLIVAR-SR3 (spring 2001) and SAZ'98 (summer 1998) stations from the STZ to the PFZ. Data are from the whole water column. STZ, STF, SAF, PFZ, as in Fig. 2; UCDW=Upper Circumpolar Deep Water; AABW=Antarctic Bottom Water; AAIW=Antarctic Intermediate Water. Circled parts 1, 2 and 3 represent surface and mesopelagic waters, 4 and 5 intermediate and bottom waters.

Clearly, silicate, alkalinity and nitrate all show correlative behaviour with Ba, but to variable extents. In the following, we assess this via a multiple regression approach.

4.2. Multiple regressions

We applied a multiple regression analysis to assess the relative weight of the above mentioned different nutrient parameters combined with other independent variables, in predicting the Ba distribution. Best subset regressions were used to search for those combinations of independent variables (silicate, nitrate, alkalinity, oxygen, temperature, salinity) providing the best prediction of the dependent variable Ba_d . To that purpose two statistics

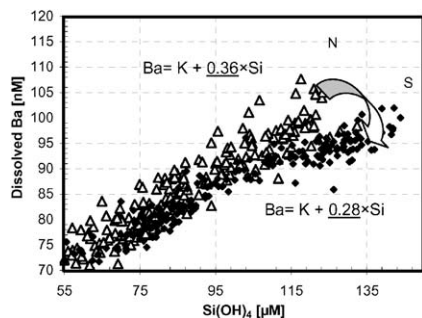


Fig. 6. Dissolved Ba (nM) versus silicate (μM) for CLIVAR-SR3 (spring 2001) stations from Subtropical Front (STF) to Antarctic Zone (AZ); data from Jacquet et al. (2004). Only intermediate and deep waters (potential densities >27.35) are considered. Empty triangles and black diamonds represent stations respectively north and south of the PF ($\sim 54^\circ\text{S}$); equations indicate the southward decrease of the slope of the Ba vs. Si regression at these two groups of stations.

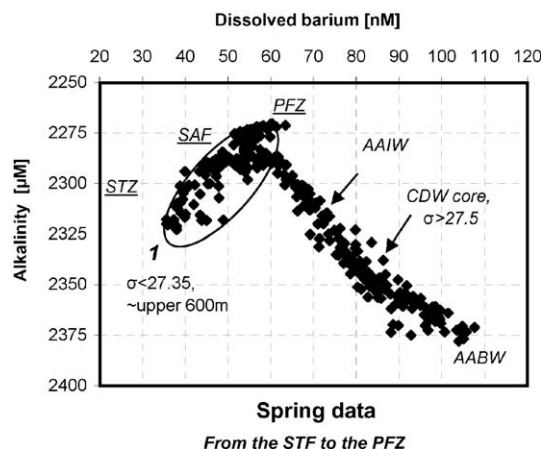


Fig. 7. Dissolved Ba (nM) versus alkalinity (μM) for CLIVAR-SR3 (spring 2001) stations from STF to AZ. Circled part 1 represents surface and mesopelagic waters. PFZ, SAF, STZ, AAIW: as in Fig. 2. CDW=Circum Polar Deep Water.

were used: (i) the adjusted R^2 , providing a measure of how well the regression model describes the data, taking into account the number of independent variables, and (ii) the t -statistic which tests the null hypothesis that the partial regression coefficient for each independent variable is zero (a variable is neglected for $p > 0.05$).

Results for CLIVAR-SR3 reveal that silicate and alkalinity are highly correlated. Though no obvious process links silicate and alkalinity, it is likely that biological synthesis of opal and carbonate and subsequent dissolution generate parallel oceanic distributions (Chan et al., 1977; Lea, 1993; Jeandel et al., 1996), thereby inducing multi-collinearity between silicate and alkalinity. This situation implies that only one of these two variables should be used in the multiple regression analysis to avoid a multi-collinearity effect, which may result in unreliable estimates of the dependent parameter (Ba_d). Since alkalinity profiles are less resolved in the deep ocean and since no alkalinity data were available for the SAZ'98 cruise, we choose to include the silicate variable, rather than alkalinity, in the multiple regression analysis.

Regression calculations using the whole CLIVAR-SR3 data set indicate that among the parameters considered, the best predictor of Ba_d is clearly Si, contributing to approximately 88% of the Ba_d variability. Despite the fact that SAZ'98 data are scarcer, best subset regressions provide similar results with Si explaining about 79% of the Ba_d variability (whole data set). When the regressions are calculated for each individual cast, different groups of stations become apparent both for CLIVAR-SR3 and SAZ'98, again with silicate explaining the major part of the Ba_d variability (Table 2; see R^2 value). It is interesting to note that these groups of stations correspond to

transition zones along the SR3 line as identified in Jacquet et al. (2004) and which are similar during spring and summer. From Table 2a,b, it appears that the partial regression coefficient for Si (i.e. the slope value) decreases from north to south (see also Fig. 6) while the intercept increases. Jeandel et al. (1996) and Monnin et al. (1999) report that waters from the upper 2000 to 3000 m of the water column south of the Polar Front are at equilibrium or oversaturated with respect to barite, in contrast to the situation north of the Polar Front where waters are undersaturated. Therefore, decreased slopes of the Ba-silicate regressions south of the PF could reflect reduced dissolution of Ba_{xs} in subsurface and intermediate waters. These results are also in general agreement with earlier work by Jeandel et al. (1996) in the Indian sector of the Southern Ocean. The latter authors also observed decreasing slopes of Ba_d vs. Si regressions from north to south of the PF and likewise concluded that differences in saturation conditions for barite between sites north and south of the front were the main reason for this. Overall, it appears that the strong Ba_d-silicate (and Ba_d-alkalinity) correlation we observe when inspecting whole water column profiles are maintained mainly by the situation in intermediate and deep waters, where dissolution of suspended biogenic barium (mainly barite), opal and carbonate parts of plankton are major processes, overprinted by hydrodynamics.

The above-discussed relationships highlight the fact that Ba_d is not controlled by the same biogeochemical processes and thermodynamic conditions controlling synthesis of opal and carbonate and their dissolution. This emphasizes the unique pseudo-nutrient behavior of barium.

4.3. Seasonality of dissolved and particulate Ba

The mesopelagic waters have been identified as being the site of barite production and its release in the water

column as discrete micro-crystals after bacterial degradation of the aggregates in which the precipitation takes place (Dehairs et al., 1980; 1997; Stroobants et al., 1991). Such a process explains why Ba_{xs} accumulation coincides with peak oxygen consumption and can be used as a proxy of organic matter remineralization (Dehairs et al., 1997). Density and Ba_{xs} gradients are sharp around 100–150 m at the bottom of the mixed layer (Figs. 3 and 4). Since sharp density gradients forming the lower boundary of the mixed layer have been reported as sites of organic aggregate and floc formation and accumulation (MacIntyre et al., 1995), the coincidence between the increase of mesopelagic Ba_{xs} and the occurrence of this density gradients is consistent with the idea that aggregates and mineralization of organic matter are involved in the process of barite formation as discussed in Cardinal et al. (2005). Furthermore, according to Collier and Edmond (1984), local uptake of Ba_d in the subsurface waters is required to maintain the mesopelagic Ba_{xs} maximum, which cannot be explained solely as a result of regeneration of carriers such as biogenic Si or SrSO₄ nor by redistributing the amount of particulate Ba present in upper mixed layer. Thus, the fact that dissolved and particulate Ba summer profiles in mesopelagic waters seem to mirror each other (Fig. 4) could indeed indicate that the latter is sustained by local Ba_d subtraction. Spring Ba_{xs} maxima, on the contrary, do not appear mirrored by significant Ba_d depletions and it is likely that this reflects differences in the turnover rates between the particulate and dissolved Ba phases. Since Ba_d concentrations exceed Ba_{xs} concentrations by a factor 100 to 1000, reflecting the faster dynamics of the latter (Dehairs et al., 1980), the time window necessary for Ba_d uptake to become detectable is likely wider than for increase in mesopelagic Ba_{xs} to become detectable. Apparently for CLIVAR-SR3 in spring, insufficient time has elapsed since the onset of

Table 2

Subset regression analysis results of Si vs. Ba_d: (a) CLIVAR-SR3 cruise (spring 2001) and (b) SAZ'98 cruise (summer 1998)

	STF	SAZ-AF/N	SAF/S-PFZ	PFZ-AZ
<i>(a) CLIVAR SR3—spring 2001</i>				
R ²	0.87	0.98	0.91	0.72
Intercept±S.E.	42.9±0.3	49.3±0.3	58.7±0.8	64.1±0.7
Slope±S.E.	0.50±0.02	0.42±0.01	0.31±0.01	0.23±0.01
<i>p</i>	<0.001	<0.001	<0.001	<0.001
<i>(b) SAZ'98—summer 1998</i>				
R ²	0.99	0.99	0.77	0.78
Intercept±S.E.	44.0±0.7	18.6±0.5	55.6±1.7	65.7±1.4
Slope±S.E.	0.56±0.11	0.52±0.01	0.32±0.04	0.21±0.03
<i>p</i>	<0.001	<0.001	<0.001	<0.001

Listed are R², intercept, slope and *p* value; see Section 4.1 for explanations. STF=Subtropical Front, SAZ=Subantarctic Zone, SAF=Subantarctic Front (N: north, S: south), PFZ=Polar Front Zone, AZ=Antarctic Zone.

the bloom for Ba_d uptake to become detectable. A time window of several months seems necessary for any Ba_d depletion to become apparent. Though Ba_{xs} has a faster turnover than Ba_d , a clear seasonal build-up of mesopelagic Ba_{xs} occurs, with summer contents systematically exceeding those in spring (Table 1 and Fig. 4; Cardinal et al., 2005). Thus, less Ba subtracted from solution in spring implies less barite formed. However, exact co-variation of Ba_{xs} and Ba_d in mesopelagic waters is not obvious since the Ba subtracted from solution is not necessarily transferred to the local barite stock, but can become associated with larger aggregates exported deeper in the water column.

4.4. Barium fluxes

To determine whether the observed summer Ba_d depletion in the mesopelagic zone can be the result of a Ba subtraction from solution during barite formation, we estimated the seasonal depletion of dissolved Ba and compared this subtraction flux with the build-up of mesopelagic Ba_{xs} as well as with deep water sediment traps derived Ba_{xs} fluxes. We calculated the subtraction of dissolved Ba required to maintain the upper 600 m water column summer depletion by applying a steady state and a non-steady state approach.

The steady state approach is performed on the summer profiles (SAZ'98) and assumes the system has been at equilibrium for some time. We apply a simple 1-D box model in which the dissolved Ba subtraction term (J , in $\mu\text{mol m}^{-2} \text{day}^{-1}$) equates the Ba_d input as sustained by vertical advection and turbulent diffusion:

$$J = \kappa(\partial Ba/\partial z)_{\text{up}} + \kappa(\partial Ba/\partial z)_{\text{down}} + W[Ba]_{\text{base}} - W[Ba]_{\text{min}} \quad (1)$$

For all the stations, the upper boundary of this box is set by the basis of the mixed layer (100 m) and the lower boundary is taken at 600 m. The turbulent diffusion coefficient k is taken constant and equal to $3 \cdot 10^{-5} \text{ m}^2 \text{ s}^{-1}$ (see Shopova et al., 1995). Turbulent diffusion transports Ba from the lower ($K(\partial Ba/\partial z)_{\text{up}}$) and upper boundaries ($K(\partial Ba/\partial z)_{\text{down}}$) of the Ba minimum layer to the center. Vertical advection moves Ba ($W[Ba]_{\text{base}}$) from the lower boundary to the center of the minimum layer and from the center ($W[Ba]_{\text{min}}$) to the upper boundary. The Ba_d minimum is located at 91 m (STF), 201 m (SAZ), 301 m (SAF) and 252 m (PFZ) (Fig. 4). For the vertical advection transport coefficient W , we use a value of $150 \cdot 10^{-5} \text{ cm s}^{-1}$ (Yaremchuck et al., 2001), the choice of which is discussed further below.

The non-steady state approach is based on the comparison of the spring (CLIVAR-SR3) and summer (SAZ'98) situations, assuming year to year variability of the onset of

the bloom to be relatively similar (see discussion in Section 2). Based on spring Ba–salinity relationships within each zone, the temporal variations of Ba_d values were corrected for ocean mixing effects, following the rationale Lourey and Trull (2001) applied to estimate seasonal nutrient utilization along the same SR3 transect:

$$\Delta Ba_{\text{bio}} = \Delta Ba_{\text{tot}} - \Delta Ba_{\text{m}} \quad (2)$$

where ΔBa_{bio} is the estimate of Ba depletion due to the biological activity, ΔBa_{tot} is the overall difference between the spring and summer barium fields, ΔBa_{m} indicates the Ba change due to ocean mixing $\Delta Ba_{\text{m}} = \Delta \text{Sal}_{\text{m}} \times (\Delta Ba / \Delta \text{Sal})$, $\Delta \text{Sal}_{\text{m}} = \text{Sal}(\text{spring}) - \text{Sal}(\text{summer})$, $\Delta Ba = \text{Ba}(\text{spring}) - \text{Ba}(\text{summer})$, $\Delta Ba / \Delta \text{Sal} = \text{slope of the Ba vs. salinity plots for surface waters (upper 100 m) in spring (i.e. supposedly waters still being little affected by biological activity)}$, used to correct for mixing. Depletions of Ba over the growth season (taken as 100 days, see discussion above) were obtained by calculating the summer versus spring difference of Ba_d contents integrated over the minimum layer (100–600 m).

Rates of Ba_d subtraction calculated via both approaches are given in Table 3a and compared with build-up of Ba_{xs} (Table 3b) in mesopelagic (i.e. seasonal build-up of Ba_{xs}) and deep waters (Table 3c; sediment trap Ba_{xs} fluxes covering the period from September 1997 to March 1998, i.e. 153 days; Cardinal et al., 2005). The build-up of Ba_{xs} in mesopelagic waters over the growth season (100 days) was obtained from the difference of mesopelagic Ba_{xs} contents integrated over the Ba_{xs} maximum layer (set equal to the Ba_d minimum layer as defined above), between summer and spring.

4.5. Comparing steady state versus non-steady state approaches to assess dissolved Ba fluxes

Overall rates of Ba_d depletions estimated via the steady state (ss) and non-steady state (n-ss) appear to converge (Table 3a). They present the same trend: fluxes are higher in the SAZ compared to STZ and decrease in the SAF and PFZ. However, differences exist. While fluxes in the STF (ss=10.5 and n-ss=11.6 $\mu\text{mol m}^{-2} \text{day}^{-1}$) and in the PFZ (ss=8.3 and n-ss=8.5 $\mu\text{mol m}^{-2} \text{day}^{-1}$) are quite similar, the steady state approach leads to lower values for the SAZ (ss=12.3 and n-ss=18.7 $\mu\text{mol m}^{-2} \text{day}^{-1}$) and the SAF (ss=6.2 and n-ss=9.3 $\mu\text{mol m}^{-2} \text{day}^{-1}$). It must be kept in mind that the vertical advection coefficient W , used in the steady state approach, is generally poorly constrained. In this study, we used a single value, but obviously, the hydrodynamic complexity along the SR3 transect, make it unlikely that W is

Table 3

Location	STF	SAZ	SAF	PFZ
<i>(a) Mesopelagic dissolved Ba subtraction</i>				
Steady state approach	10.5	12.3	6.2	8.3
Non-steady state approach	11.6	18.7	9.3	8.5
<i>(b) Mesopelagic particulate Ba build-up</i>				
Ba _{xs}	–	0.86	1.32	1.06
<i>(c) Deep water particulate Ba flux</i>				
Ba _{xs} *	–	1.50 ⁽¹⁾ 2.97 ⁽²⁾ 1.43 ⁽³⁾	0.73 ⁽⁴⁾	0.74 ⁽⁵⁾ 0.68 ⁽⁶⁾

All fluxes in $\mu\text{mol m}^{-2} \text{day}^{-1}$.

* Sediment trap derived deep water Ba_{xs} fluxes: values corrected from trapping efficiencies (estimated from ²³⁰Thex flux; Trull et al., 2001b; Cardinal et al., 2005).

Sediment trap depths: 1–1060 m, 2–2050 m, 3–3850 m, 4–3089 m, 5–800 m and 6–1580 m.

constant neither within zones nor with depth. Vertical advection coefficients reported in literature range over two orders of magnitude, from $10^{-5} \text{ cm s}^{-1}$ (e.g. Shopova et al., 1995) to $200 * 10^{-5} \text{ cm s}^{-1}$ and more (Yaremchuck et al., 2001). In this study, we use a value of $150 * 10^{-5} \text{ cm s}^{-1}$ representing the mean of the values reported by Yaremchuck et al. (2001) for the same WOCE SR3 transect. Calculation of depletion fluxes by applying a W value of $200 * 10^{-5} \text{ cm s}^{-1}$ (Yaremchuck et al., 2001) for the SAZ and SAF which are particularly marked by an unstable and complex hydrodynamical regime brings the ss and n-ss fluxes to the same level. Because of poorly constrained transport coefficients, overall, the steady state model is probably the least robust one for predicting subtraction fluxes.

4.6. Discrepancies between dissolved Ba subtraction and particulate Ba fluxes

Although the SAZ shows the highest Ba_d subtraction flux and also the highest deep-ocean Ba_{xs} flux, the mesopelagic Ba_{xs} build-up is lowest there. The PFZ, on the other hand, has the lowest Ba_d subtraction flux, the lowest deep-ocean Ba_{xs} flux (at 1580 m), but a large mesopelagic Ba_{xs} build-up (slightly lower than the one in the SAF). Trull et al. (2001b) report that carbon export to the deep ocean in the SAZ sector is larger than in the PFZ and deep-sea Ba_{xs} fluxes have been shown to follow this trend (Cardinal et al., 2005; Table 3c). Furthermore, there is an inverse latitudinal trend between deep-ocean Ba_{xs} fluxes and mesopelagic Ba_{xs} contents as discussed in Cardinal et al. (2005). These conditions potentially reflect the importance of CaCO₃ mineral ballast north of

the PF and a more intense mineralization in the mesopelagic waters in the PF where diatoms dominate (see Cardinal et al., 2005), in general agreement with the conclusions by François et al. (2002) and Klaas and Archer (2002) that CaCO₃ is the important controller of deep export flux, rather than opal.

A major issue concerning the Ba fluxes is the order of magnitude difference between mesopelagic Ba_d subtraction and Ba_{xs} build-up (Table 3a and b). Balance between Ba_{xs} gain and Ba_d deficit in mesopelagic waters is not really expected since the Ba subtracted from solution is not necessarily transferred to the local barite stock, but can become associated with larger aggregates exported to the deep ocean. This would mean that Ba subtraction fluxes have to be compared with the combined mesopelagic and the deep-ocean Ba_{xs} fluxes. However, even adding sediment trap and mesopelagic Ba fluxes does not balance the discrepancy between dissolved and particulate fluxes (Table 3a,b). As already emphasized, the turnover of particulate Ba is faster than Ba_d and this may in part explain the difference between the two fluxes. We remind that the mesopelagic Ba_{xs} inputs have been integrated over a period of ~ 3 months during the growth season. Therefore, considering the large difference in turnover dynamics of the dissolved vs. particulate Ba phases (months vs. weeks, respectively), we also looked at the temporal evolution of the Ba_{xs} signal over a shorter time interval. For the CLIVAR-SR3 cruise (spring), we have data for a station in the Antarctic Zone (60.9°S) visited twice in a time span of 17 days, providing an estimate of the mesopelagic Ba_{xs} flux over a shorter period of time (see Cardinal et al., 2005). This short term Ba_{xs} build-up integrated between 100 and 600 m amounts to $3.1 \mu\text{mol m}^{-2} \text{day}^{-1}$. Also Dehairs et al. (1997) report a short term (3 weeks; early spring) mesopelagic particulate Ba build-up of similar magnitude ($1.4 \mu\text{mol m}^{-2} \text{day}^{-1}$) for a Polar Front station in the Atlantic sector of the Southern Ocean (ANTX/6 cruise; 1992). Such values are two to seven times larger than the estimates in the present study, based on the differences between summer 1998 and spring 2001 Ba_{xs} profiles at SR3. As discussed above, this may indicate that while the mesopelagic dissolved Ba depletion reflects uptake integrated over the growth season, the Ba_{xs} stock fluctuates over a shorter time scale, tuned for instance by short term variability of primary production. However, it is unlikely that the discrepancies between dissolved and particulate fluxes are due solely to problems related to the width of the time windows over which signals are integrated. Jeandel et al. (1996) and Monnin et al. (1999) show that the ocean north of the Polar Front is undersaturated for

barite over the whole water column, in contrast to waters of the Antarctic Circumpolar Current. Therefore, dissolution of barite, the major carrier of Ba_{xs} , at depths > 1000 m is likely a main factor accounting for the discrepancies between the Ba_d subtraction fluxes and the mesopelagic and deep-ocean Ba_{xs} fluxes.

We tried to verify whether or not the Ba dissolution rates suggested by the data in Table 3a for the deep ocean are realistic. Comparing our dissolved Ba data for the CIVA-1 section at $30^\circ E$ (unpublished results and Jacquet et al., 2005a) with those for the WOCE SR-3 section at $145^\circ E$ (this study and Jacquet et al., 2004), we noticed an increase of on average 7 nM for waters deeper than 1000 m and having potential densities between 27.70 and 27.83. These are the waters that cover the depth range (i.e. about lower 3000 m of water column) undersaturated for barite (Monnin et al., 1999; Jeandel et al., 1996). Next we performed a simple calculation of dissolved Ba input in the deep sea during water mass transit between 30° and $145^\circ E$. Between the SAF and the PF, we considered water mass transport to reach 130 Sv, while from the PF to the Antarctic margin only 50 Sv are transported (Rintoul and Sokolov, 2001; Park et al., 2001). North of the PF the estimated average transit time is 5.3 years (velocity = 4.7 cm s^{-1}), while south of the PF estimated average transit time increases to 18.4 years (velocity = 1.2 cm s^{-1}). The calculated input rate of dissolved Ba to the deep ocean, then ranges between 4 (area south of PF) and $14 \mu\text{mol m}^{-2} \text{ day}^{-1}$ (SAZ and PFZ) what is similar to the values obtained for Ba subtraction in the mesopelagic area along SR-3 line. Thus, calculations suggest that the discrepancy between particulate Ba fluxes (mesopelagic build-up and deep-ocean particle flux) and dissolved Ba subtraction in the mesopelagic waters can be accounted for by intermediate-deep-ocean dissolution of particulate Ba.

5. Conclusions

Although regression analyses reveal strong similarities between dissolved Ba and silicate distributions along the WOCE SR3 line in the Southern Ocean and identify silicate as the best predictor of Ba_d , this Ba_d -silicate co-variation breaks down in surface waters. Here, Ba_d rather follows the latitudinal trend of nitrate, showing gradual decrease northward, while silicate is depleted over large parts of the SR3 section. Moreover, regression slopes of Ba_d as a function of silicate decrease from north to south, and this is particularly salient for deeper waters known to evolve from

undersaturation to oversaturation with respect to barite, across the Polar Front. These facts not only eliminate diatoms as significant consumers of Ba_d , but also corroborate barite being the main particulate Ba phase in suspended matter.

For the SAZ and PFZ, the combined seasonal build-up of particulate Ba in mesopelagic waters and deep-ocean Ba fluxes underscore estimates of dissolved Ba subtraction in mesopelagic waters. This discrepancy suggests significant dissolution of barite to occur in the deeper water column.

Acknowledgements

The authors thank the officers and crew of the R/V Aurora Australis for their efficient technical support during SAZ'98 and CLIVAR-SR3 cruises. J. Navez and L. Monin (MRAC) provided skillful assistance during sample processing and analysis. We are grateful to Marc Rosenberg (CTD team) and Bronte Tilbrook for providing and sharing data (CTD profiles and alkalinity data). Chris Rathbone and Brian Griffiths are thanked for kindly providing satellite images of bloom developments in the studied area and assistance with image interpretation. This work was conducted in the framework of AAD projects ASAC 1343 and 2242 and was supported by BELSPO, the Federal Office for Science Policy SPSPD II program on Global Change, Ecosystems and Biodiversity, Brussels, Belgium (BELCANTO II Antarctic research network; contracts A4/DD/B11, A4/DD/B13, EV/03/7A and EV/37/7A) and Vrije Universiteit Brussel (grant GOA22).

References

- Arrigo, K.R., Worthen, D., Schnell, A., Lizotte, M.P., 1998. Primary production in Southern Ocean waters. *J. Geophys. Res.* 109 (C8), 15587–15600.
- Bertram, M.A., Cowen, J.P., 1997. Morphological composition evidence for biotic precipitation of marine barite. *J. Mar. Res.* 55, 577–593.
- Bernstein, R.E., Byrne, R.H., 2004. Acantharians and marine barite. *Mar. Chem.* 68, 45–50.
- Bernstein, R.E., Byrne, R.H., Schijf, J., 1998. Acantharians: a missing link in the oceanic biogeochemistry of barium. *Deep-Sea Res.* 45, 491–505.
- Bishop, J.K.B., 1988. The barite–opal–organic carbon association in oceanic particulate matter. *Nature* 332, 341–343.
- Cardinal, D., Dehairs, F., Cattaldo, T., André, L., 2001. Geochemistry of suspended particles in the subantarctic and polar frontal zones south of Australia: constraints on export and advection processes. *J. Geophys. Res.* 106 (C12), 31637–31656.
- Cardinal, D., Savoye, N., Trull, T.W., André, L., Kopczynska, E., Dehairs, F., 2005. Particulate Ba distributions and fluxes suggest latitudinal variations of carbon mineralization in the Southern ocean. *Deep-Sea Res.* 52, 355–370.

- Chan, L.H., Drummond, D., Edmond, J.M., Grant, B., 1977. On the barium data from the Atlantic GEOSECS Expedition. *Deep-Sea Res.* 24, 613–649.
- Collier, R., Edmond, J., 1984. The trace element geochemistry of marine biogenic particulate matter. *Prog. Oceanogr.* 13, 113–199.
- Dehairs, F., Chesselet, R., Jedwab, J., 1980. Discrete suspended particles of barite and the barium cycle in the open Ocean. *Earth Planet. Sci. Lett.* 49, 528–550.
- Dehairs, F., Stroobants, N., Goeyens, L., 1991. Suspended barite as a tracer of biological activity in the Southern Ocean. *Mar. Chem.* 35, 399–410.
- Dehairs, F., Shopova, D., Ober, S., Veth, C., Goeyens, L., 1997. Particulate barium stocks and oxygen consumption in the Southern Ocean meso-pelagic water column during spring and early summer: relationship with export production. *Deep-Sea Res.* II 44 (1–2), 497–516.
- Dehairs, F., Fagel, N., Antia, A.N., Peinert, R., Elskens, M., Goeyens, L., 2000. Export production in the Bay of Biscay as estimated from barium-barite in settling material: a comparison with new production. *Deep-Sea Res.* I 47, 583–601.
- Esser, B.K., Volpe, A.M., 2002. At-sea high-resolution chemical mapping: extreme barium depletion in North Pacific surface water. *Mar. Chem.* 79 (2), 67–79.
- François, R., Honjo, S., Krishfield, R., Manganini, S., 2002. Factors controlling the flux of organic carbon to the bathypelagic zone of the ocean. *Glob. Biogeochem. Cycles* 16. doi:10.1029/2001GB001722.
- Fresnel, J., Galle, P., Gayral, P., 1979. Résultats de la microanalyse des cristaux vacuolaires chez deux Chromophytes unicellulaires marines: *Exanthemachrysis gayraliae*, *Pavlova* sp. (Prymnesiophycées, Pavlovacées). *C. R. Acad. Sc., Paris* 288D, 823–825.
- Freydier, R., Dupré, B., Polvé, M., 1995. Analysis by ICP-MS of Ba concentrations in water and rock samples. Comparison between isotope dilution and external calibration with or without internal standard. *Eur. Mass Spectrom.* 23, 301–317.
- Ganeshram, R.S., François, R., Commeau, J., Brown-Leger, S.L., 2003. An experimental investigation of barite formation in seawater. *Geochim. Cosmochim. Acta* 67 (14), 2599–2605.
- González-Muñoz, M.T., Luque, B.F., Ruiz, F.M., Chekroun, K.B., Arias, J.M., Gallego, M.R., Canamero, M.M., deLinares, C., Paytan, A., 2003. Precipitation of barite by *Myxococcus xanthus*: possible implications for the biogeochemical cycle of barium. *Appl. Environ. Microbiol.* doi:10.1128/AEM.69.9.5722-5725.2003.
- Jacquet, S.H.M., de Brauwere, A., Dehairs, F., Elskens, M., Jeandel, C., Metzl, N., Rintoul, S., Trull, T., 2005a. Comparison of dissolved barium with nutrients and physico-chemical conditions along 30°E and 145°E across the Southern Ocean. *EGU, Viena, Austria*. 24–29 April 2005.
- Jacquet, S.H.M., Dehairs, F., Cardinal, D., Navez, J., Delille, B., 2005b. Barium distribution across the Southern Ocean Frontal system in the Crozet-Kerguelen Basin. *Mar. Chem.* 95 (3–4), 149–162.
- Jacquet, S.H.M., Dehairs, F., Rintoul, S., 2004. A high resolution transect of dissolved barium in the Southern Ocean. *Geophys. Res. Lett.* 31, L14301. doi:10.1029/2004GL20016.
- Jeandel, C., Dupré, B., Lebaron, G., Monnin, C., Minster, J.F., 1996. Longitudinal distributions of dissolved barium, silica and alkalinity in the western and southern Indian Ocean. *Deep-Sea Res.* I 43 (1), 1–31.
- Klaas, C., Archer, D.E., 2002. Association of sinking organic matter with various types of mineral ballast in the deep sea: implications for the rain ratio. *Glob. Biogeochem. Cycles* 16 (4), 1116.
- Klinkenberg, H., VanBorm, W., Souren, F., 1996. A theoretical adaptation of the classical isotope dilution technique for practical routine analytical determinations by means of inductively coupled plasma mass spectrometry. *Spectrochim. Acta* 51B, 139–153.
- Klinkhammer, G.P., Chan, L.H., 1990. Determination of barium in marine waters by isotope dilution inductively coupled plasma mass spectrometry. *Anal. Chim. Acta* 232, 323–329.
- Landry, M.R., Selph, K.E., Brown, S.L., Abbott, M.R., Measures, C.I., Vink, S., Allen, C.B., Calbet, A., Christensen, S., Nolla, H., 2002. Seasonal dynamics of phytoplankton in the Antarctic Polar Front at 170°W. *Deep-Sea Res.* II 49, 1843–1865.
- Lea, D.W., 1993. Constraints on the alkalinity and circulation of glacial circumpolar deep water from benthic foraminiferal barium. *Glob. Biogeochem. Cycles* 7, 695–710.
- Lea, D.W., Boyle, E., 1989. Barium content of benthic foraminifera controlled by bottom water composition. *Nature* 338, 751–753.
- Lourey, M., Trull, T., 2001. Seasonal nutrient depletion and carbon export in the Subantarctic and Polar Frontal Zones on the Southern Ocean south of Australia. *J. Geophys. Res.* 106 (12), 31463–31487.
- MacIntyre, S., Alldredge, A.L., Gotschalk, C.C., 1995. Accumulation of marine snow at density discontinuities in the water column. *Limnol. Oceanogr.* 40, 449–468.
- Millero, F.J., Lee, K., Roche, M., 1998. Distribution of alkalinity in the surface waters of the major oceans. *Mar. Chem.* 65, 253–261.
- Monnin, C., Jeandel, C., Cattaldo, T., Dehairs, F., 1999. The marine barite saturation state of the world's ocean. *Mar. Chem.* 65, 253–261.
- Navez, J., Dehairs, F., Cattaldo, T., 1999. Isotope dilution ICP-MS measurement of barium in sea water: improvement of the accuracy with a new approach to correct for mass bias. *Colloquium Spectroscopicum Internationale XXXI*, September 5–10, 1999, Ankara, Turkey.
- Östlund, H., Craig, H., Broecker, W., Spencer, D., 1987. GEOSECS Atlantic, Pacific and Indian Ocean Expeditions, Vol 7. Shore-based Data and Graphics. NSF, Washington, DC.
- Park, Y.H., Charriaud, E., Craneguy, P., 2001. Fronts, transports, and Weddell gyre at 30°E between Africa and Antarctica. *J. Geophys. Res.* 106 (C2), 2857–2879.
- Poisson, A., Schauer, B., Brunet, C., 1990. Les rapports de campagnes à la Mer, MD53/INDIGO 3 à bord du 'Marion Dufresne', 3 janvier–27 février 1987; Pub. 87-01, Fascicule 2 269pp.; Les Publications de la Mission de Recherche de Terres Australes et Antarctiques Françaises, Paris.
- Rathbone C. and B. Griffiths. NASA ocean colour web, global 8 day mean chlorophyll composites. Feldman, G. C., C. R. McClain, Ocean Color Web, SeaWiFS Reprocessing 5, NASA Goddard Space Flight Center. Eds. Kuring, N., Bailey, S. W. <http://oceancolor.gsfc.nasa.gov/>, with graphical processing by Chris Rathbone, CSIRO Marine and Atmospheric Research, 2006.
- Rintoul, S.R., Bullister, J.L., 1999. A late winter hydrographic section from Tasmania to Antarctica. *Deep-Sea Res.* I 46, 1417–1454.
- Rintoul, S.R., Sokolov, S., 2001. Baroclinic transport variability of the Antarctic Circumpolar Current south of Australia (WOCE repeat section SR3). *J. Geophys. Res.* 106 (C2), 2815–2832.
- Rosenberg M., Rintoul S., Bray S., Curran C. and N. Johnston. Aurora Australis Marine Science Cruise AU0103, CLIVAR-SR3 Transect-Oceanographic Field Measurements and Analysis. ACE-CRC, Hobart, unpublished report.
- Rushdi, A.I., McManus, J., Collier, R.W., 2000. Marine barite and celestite saturation in seawater. *Mar. Chem.* 69 (1–2), 19–31.
- Shopova, D., Dehairs, F., Baeyens, W., 1995. A simple model of biogeochemical element distribution in the water column of the Southern Ocean. *J. Mar. Syst.* 6, 331–344.
- Sokolov, S., Rintoul, S.R., 2002. Structure of Southern Ocean fronts at 140°E. *J. Mar. Syst.* 37, 151–184.

- Sternberg, E., Jeandel, C., Robin, E., Reyss, J.-L., vanBeek, P., Souhaut, M., 2005a. Profiles of particulate barium in the Mediterranean Sea coupled to radium and strontium measurements. European Geosciences Union Meeting 2005, Vienna, Austria. *Geophys. Res. Abstracts*, vol. 7, 08745, 2005.
- Sternberg, E., Tang, D., Ho, T.-Y., Jeandel, C., Morel, F.M.M., 2005b. Barium uptake and adsorption in diatoms. *Geochim. Cosmochim. Acta* 69, 2745–2752.
- Stroobants, N., Dehairs, F., Goeyens, L., Vanderheijden, N., Van Grieken, R., 1991. Barite formation in the Southern Ocean water column. *Mar. Chem.* 35, 411–421.
- Taylor, S.R., McLennan, S.M., 1985. *The continental crust: its composition and evolution*. Blackwell Scientific Publications. 312 pp.
- Trull, T., Rintoul, S.R., Hadfield, M., Abraham, R., 2001a. Circulation and seasonal evolution of polar waters south of Australia: implication for iron fertilization of the Southern Ocean. *Deep-Sea Res. II* 48, 2439–2466.
- Trull, T.W., Bray, S.G., Manganini, S.J., Honjo, S., François, R., 2001b. Moored sediment trap measurements of carbon export in the Subantarctic and Polar Frontal Zones of the Southern Ocean, south of Australia. *J. Geophys. Res.* 106 (C12), 31,489–31,509.
- Yaremchuck, M., Bindoff, N.L., Schröter, J., Nechaev, D., Rintoul, S. R., 2001. On the zonal and meridional circulation and ocean transport between Tasmania and Antarctica. *J. Geophys. Res.* 106 (2), 2795–2814.